The abundant DNA adduct N^7-methyl deoxyguanosine contributes to miscoding during replication by human DNA polymerase η

Received for publication, April 19, 2019, and in revised form, May 16, 2019 Published, Papers in Press, May 17, 2019, DOI 10.1074/jbc.RA119.008986

Olive J. Njuma, Yan Su, and F. Peter Guengerich[1]

From the Department of Biochemistry, Vanderbilt University School of Medicine, Nashville, Tennessee 37232-0146

Edited by Patrick Sung

Aside from abasic sites and ribonucleotides, the DNA adduct N^7-methyl deoxyguanosine (N^7-CH_3 dG) is one of the most abundant lesions in mammalian DNA. Because N^7-CH_3 dG is unstable, leading to deglycosylation and ring-opening, its miscoding potential is not well-understood. Here, we employed a 2′-fluoro isostere approach to synthesize an oligonucleotide containing an analog of this lesion (N^7-CH_3 2′-F dG) and examined its miscoding potential with four Y-family translesion synthesis DNA polymerases (pols): human pol (hpol) η, hpol κ, and hpol ι and Dpo4 from the archaeal thermophile *Sulfolobus solfataricus*. We found that hpol η and Dpo4 can bypass the N^7-CH_3 2′-F dG adduct, albeit with some stalling, but hpol κ is strongly blocked at this lesion site, whereas hpol ι showed no distinction with the lesion and the control templates. hpol η yielded the highest level of misincorporation opposite the adduct by inserting dATP or dTTP. Moreover, hpol η did not extend well past an N^7-CH_3 2′-F dG:dT mispair. MS-based sequence analysis confirmed that hpol η catalyzes mainly error-free incorporation of dC, with misincorporation of dA and dG in 5–10% of products. We conclude that N^7-CH_3 2′-F dG and, by inference, N^7-CH_3 dG have miscoding and mutagenic potential. The level of misincorporation arising from this abundant adduct can be considered as potentially mutagenic as a highly miscoding but rare lesion.

DNA is constantly damaged by both endogenous (*e.g.* reactive oxygen species and SAM) and exogenous (*e.g.* polycyclic hydrocarbons and heterocyclic amines) sources (1). Examples of DNA damage include DNA adducts (*e.g.* alkylated and oxidized bases), single strand breaks, double strand breaks, DNA mismatches, abasic sites, and pyrimidine dimers (2). Such damage, if not repaired, can cause deleterious outcomes (*e.g.* stalled replication and miscoding events leading to cancer, teratogenesis, and cardiovascular disease) (3–6). Alkylating agents used in treatment of malignancies (such as cyclophosphamide, temozolomide, and melphalan) have been associated with causing cancers (*e.g.* lymphomas, malignant gliomas, and lung and ovarian cancers) (7–11).

The nitrogen and oxygen atoms of DNA bases are reactive toward several known alkylating agents, producing different types of DNA adducts (12, 13). Exposure of DNA to methylating agents forms several modified bases, including N^3-methyl deoxyadenosine, N^7-methyl deoxyguanosine (N^7-CH_3 dG),[2] O^6-methyl deoxyguanosine (O^6-CH_3 dG), and O^4-methyl (deoxy)thymidine (13). O^6-CH_3 dG and O^4-methyl (deoxy)thymidine are minor adducts but are highly cytotoxic and mutagenic; the mutagenicity of the abundant N^7-CH_3 dG and N^3-methyl deoxyadenosine adducts is not known (14, 15).

The N7 atom of deoxyguanosine is the most nucleophilic site in DNA and is susceptible to alkylation, forming various N^7-alkyl deoxyguanosine adducts (13, 16, 17). These adducts include N^7-CH_3 dG, N^7-ethyl deoxyguanosine, and N^7-benzyl deoxyguanosine (13, 18, 19). The deoxyguanosine adduct formed with the 8,9-*exo*-epoxide of the hepatocellular carcinogen aflatoxin B_1 is highly mutagenic, causing GC to TA transversion mutations (6, 19).

N^7-CH_3 dG has been detected as the major DNA adduct formed by methylating agents and is the most abundant lesion in DNA aside from abasic sites (1, 20, 21) and ribonucleotides (22, 23), present in lymphocytes at levels of 14 adducts/10^7 normal nucleotides for nonsmokers and 25 adducts/10^7 nucleotides in smokers (24). Endogenous methylation of DNA, apparently from SAM, has been identified as the primary source of N^7-CH_3 dG adducts observed in the livers of untreated rats (25, 26).

The miscoding and mutagenic potentials of the resulting depurination (*i.e.* abasic sites) and ring-opened (*i.e.* N^7-CH_3 formamidopyrimidine (FAPY) dG) products of N^7-CH_3 dG have been extensively studied (27–31). The miscoding potential of N^7-CH_3 dG itself is not understood. Despite its abundance, N^7-CH_3 dG has been largely ignored in favor of other alkylated bases due to its instability to depurination and base-catalyzed ring-opening. It has been assumed that N^7-CH_3 dG is not mis-

This work was supported, in whole or in part, by National Institutes of Health Grants R01 ES010546 (to F. P. G.) and T32 ES007028 (to F. P. G. and O. J. N.). The authors declare that they have no conflicts of interest with the contents of this article. The content is solely the responsibility of the authors and does not necessarily represent the official views of the National Institutes of Health.

This article contains Scheme S1, Tables S1–S6, and Figs. S1–S12.

[1] To whom correspondence should be addressed: Dept. of Biochemistry, Vanderbilt University School of Medicine, 638 Robinson Research Bldg., 2200 Pierce Ave., Nashville, TN 37232-0146. Tel.: 615-322-2261; Fax: 615-343-0704; E-mail: f.guengerich@vanderbilt.edu.

[2] The abbreviations used are: N^7-CH_3 dG, N^7-methyl deoxyguanosine; N^7-CH_3 2′-F dG, N^7-methyl 2′-fluoro deoxyguanosine; 2′-F dG, 2′-fluoro deoxyguanosine; FAM, 6-carboxyfluorescein; FAPY, formamidopyrimidine; FPG, formamidopyrimidine DNA glycosylase; pol, DNA polymerase; hpol, human pol; O^6-CH_3 dG, O^6-methyl deoxyguanosine; UDG, uracil-DNA glycosylase; CID, collision-induced dissociation; ESI, electrospray ionization.

© 2019 Njuma et al. Published under exclusive license by The American Society for Biochemistry and Molecular Biology, Inc.

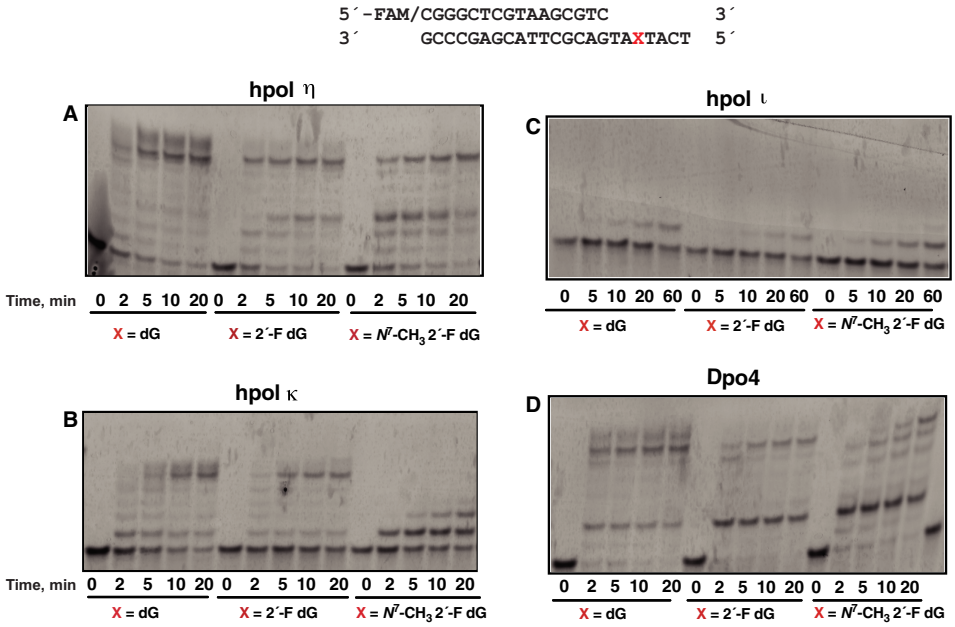

Figure 1. Bypass across and extension past dG, 2′-F dG, and N^7-CH_3 2′-F dG. *A*, hpol η; *B*, hpol κ; *C*, hpol ι; *D*, Dpo4. The sequences of the template and primer are shown at the *top*. Reactions contained 200 nM FAM-labeled primer–template oligonucleotide complex, 250 μM dNTPs, and 20 nM enzyme, except for pol ι (40 nM). Reactions were done at 37 °C for 2, 5, 10, 20, and 60 min.

coding because it should not alter the canonical Watson–Crick hydrogen-bonding pattern (32). However, the techniques that were used to reach this conclusion were not very sensitive compared with modern methods, and only a few model DNA polymerases were considered (21, 33).

In 1961, Lawley and Brookes (34) proposed that alkylation at the guanine N7 position might induce mispairing due to its lowering of the pK_a of the N1 position from 9 to 7, favoring rare tautomers (17, 34–36). Even a low level of misincorporation across a very abundant lesion would be similar in risk to a highly miscoding but rare lesion.

Koag *et al.* (37) employed an isosteric fluorine transition-state destabilization approach to stabilize the glycosidic bond, to avoid depurination and mild deprotection conditions to prevent ring-opening to N^7-CH_3 FAPY dG. Although the lesion inhibited catalysis by pol β, replication was reported to be highly accurate (*i.e.* dCTP was inserted opposite N^7-CH_3 dG) (37). We used this 2′-fluoro analog, N^7-CH_3 2′-F dG, and analyzed its miscoding potential with several Y-family translesion synthesis polymerases (human pols (hpols) η, κ, and ι and *Sulfolobus solfataricus* Dpo4). N^7-CH_3 2′-F dG caused miscoding with hpol η and has mutagenic potential, which we infer is the case with N^7-CH_3 dG.

Results

Synthesis of 2′-F dG- and N^7-CH_3 2′-F dG–containing oligonucleotides

A fluorine analog of the lesion (N^7-CH_3 2′-F dG) was prepared by modifying the approach of Lee *et al.* (32) (Scheme S1 and Figs. S1–S4). The 23-mer oligonucleotides were characterized by LC-ESI-MS (Figs. S5*B* and S6*A*). The N^7-CH_3 2′-F dG–containing oligonucleotide was resistant to cleavage by FPG glycosylase, further confirming its identity as the intact lesion rather than the ring-opened N^7-CH_3 FAPY 2′-F dG oligonucleotide, which is a substrate for this glycosylase (Fig. S6*B*). Following alkaline treatment to form the FAPY lesion, FPG glycosylase cleaved the lesion (Fig. S6*B*). We conclude that the desired N^7-CH_3 2′-F dG lesion was present and that the two potential problems, depurination and ring-opening, had been avoided.

Primer extension past dG, 2′-F dG, and N^7-CH_3 2′-F dG by Y-family DNA polymerases

Four Y-family DNA polymerases were studied (hpol η, hpol κ, hpol ι, and Dpo4). hpol η and Dpo4 were the most effective of these in producing full-length extension products, although they both stalled following the P + 3 and P + 2 products, respectively (Fig. 1, *A* and *D*). In contrast, hpol κ stalled at the adduct (Fig. 1*B*), and hpol ι showed no distinction between the control templates and the adduct, stalling before the dG templates and the lesion (Fig. 1*C*).

To determine the insertions across the adduct, primer extension experiments were done with individual dNTPs. hpol η and Dpo4 were highly error-prone with all three templates examined (Fig. 2, *A* and *D*). Dpo4 did not misincorporate dATP in the 2′-F dG control. In contrast with these two polymerases, hpol κ and hpol ι incorporated only the correct dCTP for all three templates under the same conditions (Fig. 2, *B* and *C*), and these two polymerases were not examined further. Rates for dCTP insertion by hpol κ were estimated (in single-nucleotide incorporation experiments) to be 1.9 min^{-1} for dG , 1.4 min^{-1} for 2′-F dG, and 0.9 min^{-1} for N^7-CH_3 2′-F dG (*i.e.* there was a ~2-fold reduction in the rates when hpol κ encountered the lesion). For hpol ι, the rates of insertion of dCTP across the templates were 0.51 min^{-1} for dG, 0.56 min^{-1} for 2′-F dG, and 0.47 min^{-1} for N^7-CH_3 2′-F dG. Thus, the rates when hpol ι encountered the lesion were comparable with the control templates.

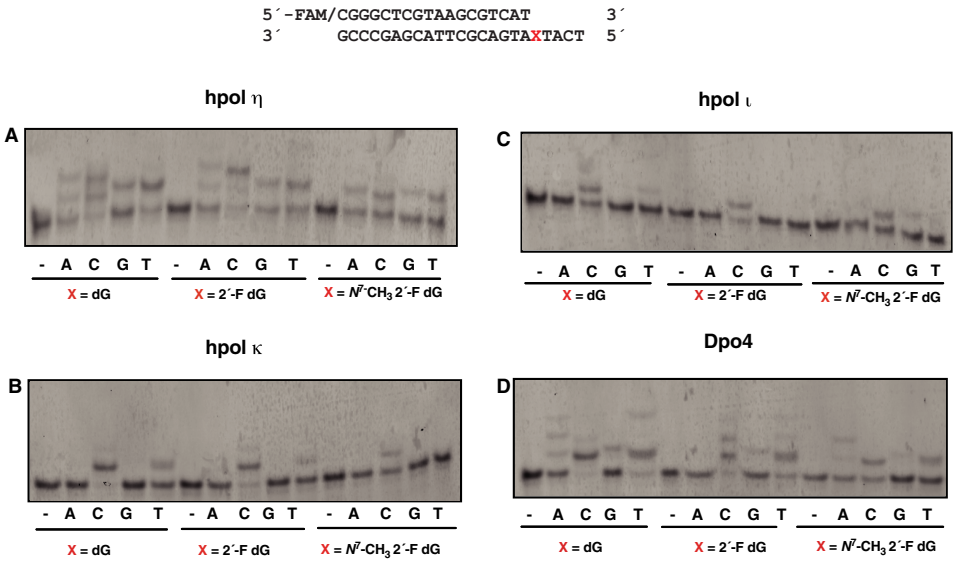

Figure 2. Single-nucleotide incorporation opposite dG, 2′-F dG, and N^7-CH_3 2′-F dG. *A*, hpol η; *B*, hpol κ; *C*, hpol ι; *D*, Dpo4. The sequences of the template and primer are shown at the *top*. Reactions were conducted with 120 nM FAM-labeled primer–template oligonucleotide complex, 250 μM dNTPs, and 5 nM enzyme except for pol ι (10 nM). Reactions were conducted at 37 °C for 10 min.

Steady-state kinetics of individual dNTP insertion opposite dG, 2′-F dG, and N^7-CH_3 2′-F dG by hpol η and Dpo4

Steady-state kinetic analysis was performed for hpol η and Dpo4 (Tables 1 and 2). The catalytic efficiencies and misincorporation frequencies for dG and 2′-F dG were comparable, as noted previously (38), suggesting that fluorine had little or no impact on polymerase recognition. With all three templates, hpol η preferred to insert dCTP relative to other dNTPs (Table 1 and Fig. 3). However, there was a 2-fold lower efficiency for incorporation of dCTP at the N^7-CH_3 2′-F dG lesion compared with dG and 2′-F dG. The efficiency for misinsertion of dATP was similar for all three templates, but the misinsertion frequency ~2-fold higher with N^7-CH_3 2′-F dG (Table 1 and Figs. 3 and S7). The catalytic efficiency for dGTP misincorporation was ~3-fold lower for the N^7-CH_3 2′-F dG lesion (Table 1 and Fig. 4). The efficiency for dTTP misincorporation was 3.5-fold greater for the N^7-CH_3 2′-F dG lesion compared with the control templates, and the misincorporation frequency was 5- and 11-fold higher relative to dG and 2′-F dG (Table 1 and Fig. 4). Thus, the misincorporation frequency for N^7-CH_3 2′-F dG was in the order dTTP > dATP > dGTP, ranging from 1 to 4% (Figs. S8 and S9).

Dpo4 preferentially inserted dCTP opposite N^7-CH_3 2′-F dG (Table 2). There was a 4-fold lower efficiency for insertion across the lesion compared with 2′-F dG (Figs. S8 and S9). The efficiencies for incorporating other dNTPs were in the order dATP > dTTP > dGTP (Table 2).

Steady-state kinetics of post-lesion incorporation of individual dNTPs opposite 2′-F dG or N^7-CH_3 2′-F dG by hpol η

Steady-state insertion kinetics provides information on dNTP insertion across a lesion but does not provide information about extension past the lesion. Steady-state kinetics were done for further extension after the correct bp (N^7-CH_3 2′-F dG:dC) and a mispair (N^7-CH_3 2′-F dG:dT). dT was used as the misincorporated base opposite the lesion because it showed the greatest misincorporation frequency in the steady-state insertion kinetics with hpol η (Table 1). With the mispairs (2′-F dG:dT and N^7-CH_3 2′-F dG:dT), only dATP was incorporated opposite the next residue (dT) (Fig. S10). The efficiency of hpol η for incorporating dATP past the mispair was ~4-fold lower for the lesion N^7-CH_3 2′-F dG than 2′-F dG, indicating some resistance to extension past the mispair (Table 3 and Fig. 5). On the other hand, the efficiency of hpol η for inserting dATP past the N^7-CH_3 2′-F dG:dC bp was 21-fold higher than the 2′-F dG:dC control, indicating that the correct pair was preferentially extended past the lesion. For the 2′-F dG control and lesion, dCTP had a similar efficiency of misincorporation past the correct pair. Finally, dTTP was misincorporated with a 6-fold higher efficiency for the lesion than the 2′-F dG control (Table 3 and Fig. 5).

LC-MS/MS sequence analysis of extension products formed by hpol η and Dpo4

We introduced a dT:dU mismatch upstream of the site of dNTP addition to utilize uracil-DNA glycosylase (UDG) to cut the extension products for analysis by LC-MS/MS. Replication of the unmodified oligonucleotide gave only error-free products, as reported elsewhere (38). Replication across the lesion by Dpo4 also gave only error-free products, in support of the results of steady-state insertion kinetics (Table 4). hpol η replicated through the lesion in both an error-free and an error-prone manner, resulting in three main products (Table 5). The first product corresponded to error-free products (*i.e.* *m/z* 934.3: 5′-pTCATGA, *m/z* 1086.3: 5′-pTCATGAT, and *m/z* 613.2: 5′-pTCAT) Figs. S11 and S12. The second corresponded to misincorporation of dA (*m/z* 934.3: 5′-pTACTGA and *m/z* 1086.3: 5′-pTAGTCAT), and the third corresponded to misincorporation of dG (*m/z* 1086.3: 5′-pTGATCAT) (Figs. S9 and S10). The CID spectra of the products matched the predicted CID spectra of the sequences (Tables S1–S6).

Table 1

Steady-state kinetics of single nucleotide insertion opposite dG, 2′-F dG, and N^7-CH_3 2′-F dG by hpol η

The oligonucleotides used were as follows,

5′-FAM-CGGGCTCGTAAGCGTCAT- 3′
3′ -GCCCGAGCATTCGCAGTA**X**TACT-5′

where **X** represents dG, 2′-F dG, or N^7-CH_3 2′-F dG.

Template base	dNTP	k_{cat}	K_m	k_{cat}/K_m	f^a
		min^{-1}	μM	$\mu M^{-1}\,min^{-1}$	
dG	dCTP	2.65 ± 0.11	0.45 ± 0.13	5.9 ± 1.7	1
2′-F dG	dCTP	1.77 ± 0.05	0.23 ± 0.06	7.7 ± 2.0	1
N^7-CH_3 2′-F dG	dCTP	1.65 ± 0.04	0.43 ± 0.07	3.8 ± 0.6	1
dG	dATP	0.76 ± 0.06	12 ± 5	0.06 ± 0.03	0.01
2′-F dG	dATP	1.1 ± 0.1	19 ± 6	0.06 ± 0.03	0.01
N^7-CH_3 2′-F dG	dATP	0.97 ± 0.04	14 ± 2	0.07 ± 0.01	0.018
dG	dGTP	0.65 ± 0.05	4.0 ± 1.7	0.16 ± 0.07	0.027
2′-F dG	dGTP	0.84 ± 0.06	2.7 ± 1.2	0.31 ± 0.14	0.040
N^7-CH_3 2′-F dG	dGTP	0.40 ± 0.06	7.5 ± 6.3	0.05 ± 0.04	0.013
dG	dTTP	1.42 ± 0.14	32 ± 11	0.04 ± 0.01	0.0068
2′-F dG	dTTP	0.96 ± 0.10	38 ± 15	0.03 ± 0.01	0.0033
N^7-CH_3 2′-F dG	dTTP	0.62 ± 0.05	4.6 ± 2.2	0.14 ± 0.07	0.037

[a] Misincorporation frequency $f = (k_{cat}/K_m)_{incorrect}/(k_{cat}/K_m)_{correct}$.

Table 2

Steady-state kinetics of single nucleotide insertion opposite dG, 2′-F dG, and N^7-CH_3 2′-F dG by *S. solfataricus* Dpo4

The oligonucleotides used were as follows,

5′-FAM-CGGGCTCGTAAGCGTCAT- 3′
3′-GCCCGAGCATTCGCAGTA**X**TACT-5′

where **X** represents dG, 2′-F dG, and N^7-CH_3 2′-F dG.

Template base	dNTP	k_{cat}	K_m	k_{cat}/K_m	f^a
		min^{-1}	μM	$\mu M^{-1}\,min^{-1}$	
dG	dCTP	158 ± 8	1.99 ± 0.41	79 ± 17	1
2′-F dG	dCTP	115 ± 2	0.30 ± 0.03	383 ± 39	1
N^7-CH_3 2′-F dG	dCTP	2.88 ± 0.10	0.03 ± 0.01	96 ± 20	1
dG	dATP	0.36 ± 0.03	14 ± 6	0.03 ± 0.01	0.0004
2′-F dG	dATP	ND[b]	ND	ND	ND
N^7-CH_3 2′-F dG	dATP	0.24 ± 0.02	9.8 ± 5.1	0.03 ± 0.02	0.0003
dG	dGTP	0.41 ± 0.04	29 ± 10	0.014 ± 0.005	0.0002
2′-F dG	dGTP	0.40 ± 0.03	21 ± 7	0.019 ± 0.007	0.0002
N^7-CH_3 2′-F dG	dGTP	0.11 ± 0.01	24 ± 21	0.01 ± 0.01	0.0001
dG	dTTP	1.38 ± 0.36	76 ± 36	0.018 ± 0.010	0.0002
2′-F dG	dTTP	0.93 ± 0.16	44 ± 16	0.021 ± 0.009	0.0001
N^7-CH_3 2′-F dG	dTTP	0.42 ± 0.04	16 ± 5	0.026 ± 0.009	0.0003

[a] Misincorporation frequency $f = (k_{cat}/K_m)_{incorrect}/(k_{cat}/K_m)_{correct}$.
[b] ND, not detected. DNA incorporation was below limits of quantitation ($v < 0.002$ min^{-1}).

To confirm these assignments, mass spectra of commercial oligonucleotide standards with these sequences were compared with those of the observed products and were nearly identical. No products were observed containing the misincorporation of dT seen in the insertion kinetics experiments (Table 1). Relative areas were calculated for each product on the basis of the intensity of distinguishing CID ions (*e.g.* a_3-B_3 ions distinguish the error-free product from the product with misincorporation of dA). The yields of the observed products were estimated to be 85% for error-free bypass, 10% for misincorporation of dA, and 5% for misincorporation of dG (Table 4).

Discussion

Alkylation of DNA was first described in 1960 (20, 39), and the N7 atom of dG has long been known to be a major site of damage (34). The change in the pK_a of the N1 atom (from 9 to 7) upon N^7-methylation (34) was considered to be a potential reason for miscoding, evoking the original postulate of rare tautomer involvement in miscoding proposed by Watson and Crick (41). Due to this issue, one cannot consider an approach with 7-deaza dG for studying N^7-alkyl dG miscoding, which would not reflect the electronic properties of the adduct. For discussion of the early studies on different alkylated bases and the development of a major role for O^6-alkyl dG adducts in mutagenesis and carcinogenesis, see Lawley (39). Although O^6-alkyl dG lesions are recognized to be important, the role of dG N^7-alkylation has remained unclear. Some early studies concluded that N^7-CH_3 dG was not miscoding (39, 42), but the results of these studies are compromised by several issues, including the sensitivity of the assays in detecting miscoding, the lack of mammalian and microbial translesion DNA polymerases, and the lability of N^7-CH_3 dG. In 2009, Boysen *et al.* (21) concluded that there was no evidence for miscoding by N^7-CH_3 dG, although the authors suggested the 2′-F isostere approach we used here to address the issue. Lee and associates (37) used N^7-CH_3 2′-F dG with pol β and concluded that it was not miscoding but did not present limits of detection or utilize sensitive methods.

N^7-Alkyl dG adducts are of particular interest because of their high endogenous levels and also high levels following exposure to alkylating agents (21, 39, 43, 44). N^7-Alkyl dG

ASBMB

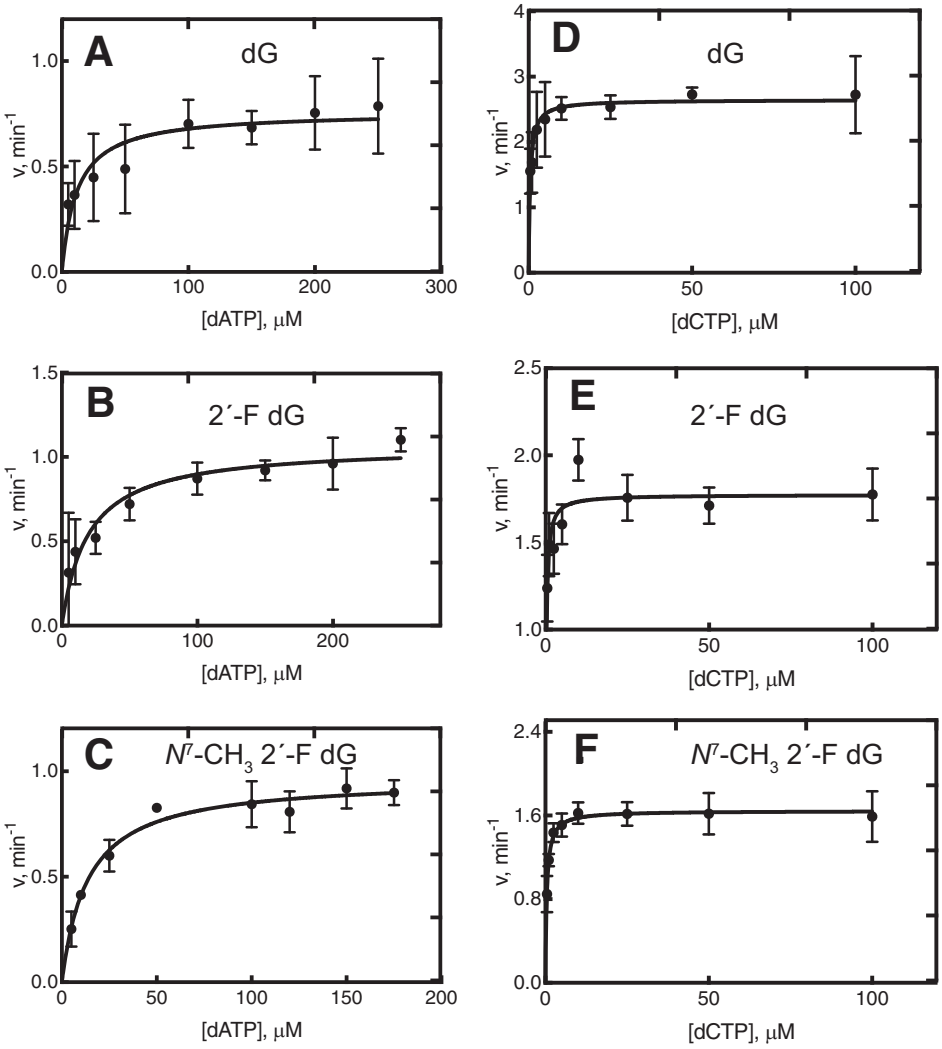

Figure 3. Steady-state kinetic analysis of individual dATP and dCTP insertions by hpol η. Reactions contained templates dG (*A* and *D*), 2′-F dG (*B* and *E*), and N^7-CH_3 2′-F dG (*C* and *F*) at position **X** in the sequences 5′-CGGGCTCGTAAGCGTCAT-3′ and 3′-GCCCGAGCATTCGCAGTA**X**TACT-5′. Reactions were done at 37 °C for 5–10 min by incubating 120 nM primer–template oligonucleotide complex. For different *panels*, different hpol η concentrations were used as indicated. For *A*, *B*, *C*, and *F*, 5 nmol of enzyme was used, and the reaction was done for 5 min, with varying concentrations of dATP and dCTP. In the *D* and *E*, 2.5 nmol of enzyme was used, and the reaction was conducted for 5 min, with varying concentrations of dATP and dCTP. Fitting was to a hyperbolic equation in GraphPad Prism version 8.0, and k_{cat} and K_m values are presented in Table 1.

adducts are found at the highest levels not only after exposure to methylating agents but with other alkylating agents as well (17, 39, 44, 45). Several examples of N^7-alkyl dG adducts are found in laboratory animals and humans not knowingly exposed to exogenous agents, including N^7-(2-hydroxy)ethyl dG, N^7-(2-oxoethyl) dG, and N^7-ethyl dG (44), but the origins of these adducts are not known. Although the levels of ribonucleotides and abasic sites have been reported to be higher than those of N^7-CH_3 dG, they are rapidly repaired by multiple pathways (22, 23), and the steady-state levels in cells are less than those of N^7-CH_3 dG (43).

The base-catalyzed imidazole ring opening of guanyl N^7-alkyl adducts has been recognized for many years. As pointed out by Gates *et al.* (17), N^7-CH_3 dG is not unusually unstable, and at neutral pH, ring-opening is very slow; even at pH 8.9, the half-life is 9.8 h (46–49). Although there was original uncertainty about the multiple forms of N^7-CH_3 FAPY dG seen in chromatography, ^{15}N NMR studies demonstrated that the site of the formyl group did not change (46) and that the adduct exists in slowly equilibrating rotomeric forms. Studies with rat liver and bladder DNA reported that levels of N^7-CH_3 dG decreased faster than those of the FAPY product, and levels of the two adducts were similar after 3–9 days (50, 51). However, Den Engelse *et al.* (49) reported only very low levels of the FAPY formed in rat liver following treatment with methylating agents. Some of the discrepancy may be due to the broadness of the N^7-CH_3 FAPY dG peaks, affecting both the resolution and the sensitivity (46, 49, 50, 52). In the report of Den Engelse *et al.* (49), no N^7-CH_3 FAPY dG adducts were detected in rat liver (<0.5% of N^7-CH_3 dG) up to 3 days after treatment with [^{14}C]dimethylnitrosamine. Even in the report of Kadlubar *et al.* (51), the level of N^7-CH_3 FAPY dG did not reach the level of N^7-CH_3 dG (in the rat bladder epithelium) until 9 days after treatment with [^{14}C]-methylnitrosourea. In considering all of this information, we conclude that the level of N^7-CH_3 dG is considerable and that

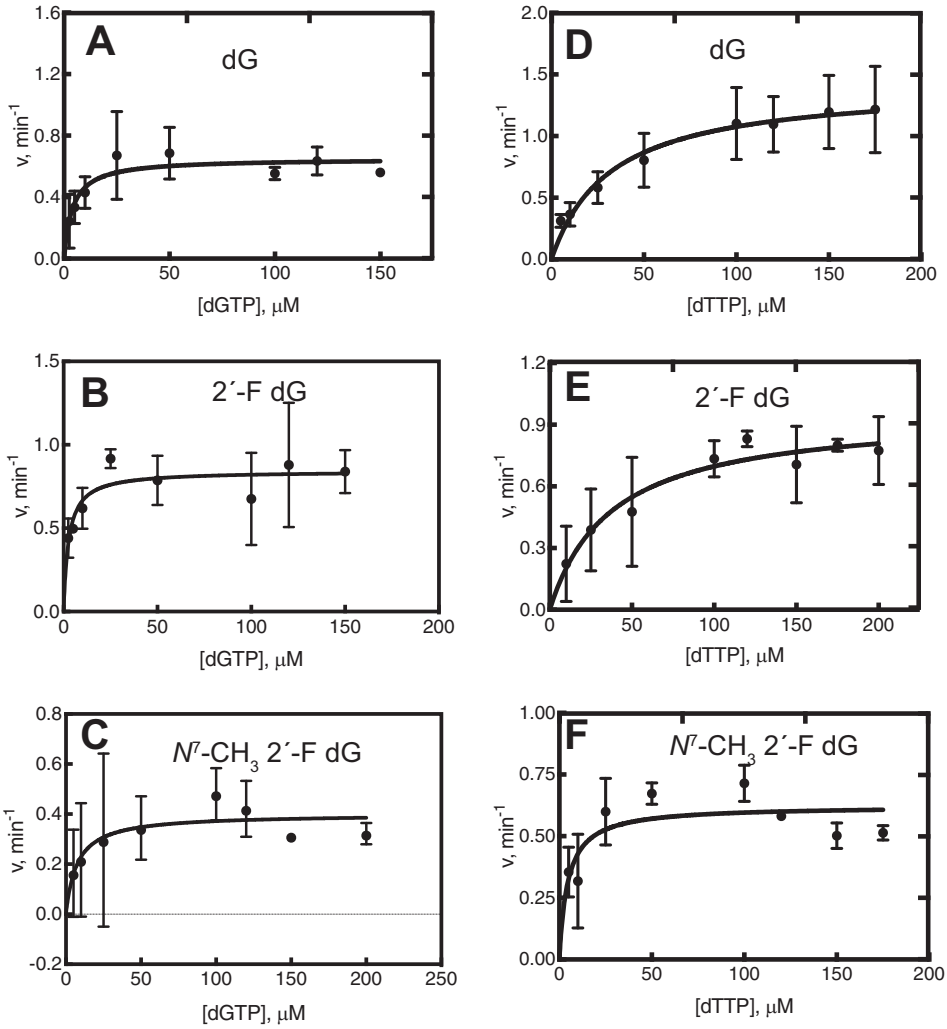

Figure 4. Steady-state kinetic analysis of individual dGTP and dTTP insertions by hpol η. Reactions contained templates dG (*A* and *D*), 2′-F dG (*B* and *E*), and N^7-CH_3 2′-F dG (*C* and *F*) at position X in the sequences 5′-CGGGCTCGTAAGCGTCAT-3′ and 3′-GCCCGAGCATTCGCAGTA**X**TACT-5′. Reactions were done at 37 °C for 5–10 min by incubating 120 nM primer–template DNA complex with varying concentrations of hpol η. For *A*, *B*, and *C*, 8 nmol of hpol η was used, and the reaction was done for 10 min. In the case of *D*, we used 8 nmol of hpol η was used, and the reaction was done for 5 min; for *E*, 10 nmol of hpol η was used, and the reaction was conducted for 5 min; and for *F*, 5 nmol of hpol η was used, and the reaction was conducted for 5 min, varying concentrations of dGTP and dTTP. Fitting was to a hyperbolic equation in GraphPad Prism version 8.0, and k_{cat} and K_m values are presented in Table 1.

Table 3

Steady-state kinetics of single nucleotide extension past 2′-F dG:dC, 2′-F dG:dT and N^7-CH_3 2′-F dG:dC, and N^7-CH_3 2′-F dG:dT base pairs by hpol η

The oligonucleotides used were as follows,

5′-FAM-CGGGCTCGTAAGCGTCATC- 3′
3′-GCCCGAGCATTCGCAGTA**X**TACT-5′

5′-FAM-CGGGCTCGTAAGCGTCATT- 3′
3′-GCCCGAGCATTCGCAGTA**X**TACT-5′

where **X** represents 2′-F dG and N^7-CH_3 2′-F dG.

Template base	Pairing	dNTP	k_{cat}	K_m	k_{cat}/K_m
			min^{-1}	μM	$\mu M^{-1} min^{-1}$
2′-F dG	Mispair	dATP	1.1 ± 0.1	4.2 ± 1.2	0.26 ± 0.08
N^7-CH_3 2′-F dG		dATP	0.49 ± 0.04	7.1 ± 2.4	0.07 ± 0.02
2′-F dG	Correct	dATP	1.1 ± 0.1	15 ± 3	0.07 ± 0.02
N^7-CH_3 2′-F dG		dATP	2.1 ± 0.1	1.4 ± 0.3	1.5 ± 0.3
2′-F dG	Correct	dCTP	0.95 ± 0.06	5.5 ± 2.2	0.17 ± 0.07
N^7-CH_3 2′-F dG		dCTP	0.75 ± 0.03	4.6 ± 1.1	0.16 ± 0.04
2′-F dG	Correct	dGTP	2.1 ± 0.06	6.9 ± 1.0	0.3 ± 0.1
N^7-CH_3 2′-F dG		dGTP	0.97 ± 0.03	3.8 ± 0.7	0.26 ± 0.1
2′-F dG	Correct	dTTP	1.0 ± 0.1	3.4 ± 0.7	0.3 ± 0.10
N^7-CH_3 2′-F dG		dTTP	1.6 ± 0.1	0.96 ± 0.47	1.7 ± 0.8

```
5′-FAM/CGGGCTCGTAAGCGTCATC      3′
3′      GCCCGAGCATTCGCAGTAXTACT 5′

5′-FAM/CGGGCTCGTAAGCGTCATT      3′
3′      GCCCGAGCATTCGCAGTAXTACT 5′
```

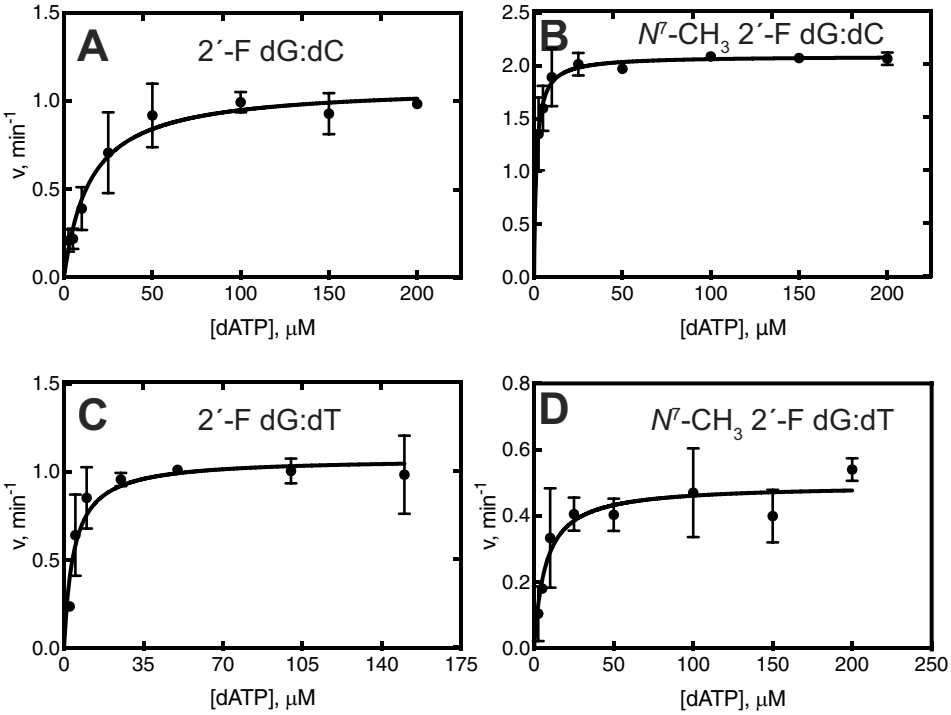

Figure 5. Steady-state kinetic analysis of dATP extension by hpol η. *A*, 2′-F dG:dC; *B*, N^7-CH$_3$ 2′-F dG:dC; *C*, 2′-F dG:dT; *D*, N^7-CH$_3$ 2′-F dG:dT bp. The sequences of the template and primer are shown at the *top*. Reactions were done at 37 °C for 5–10 min by incubating 120 nM primer–template oligonucleotide complex, 5–10 nM hpol η, and varying concentrations of dNTPs.

Table 4

LC-ESI-MS/MS analysis of full-length extension products across N^7-CH$_3$ 2′-F dG by hpol η

The oligonucleotides used were as follows,

5′-FAM-CGGGCTCGTAAGCGTCUT- 3′
3′-GCCCGAGCATTCGCAGTA**X**TACT-5′

where **X** represents 2′-F dG and N^7-CH$_3$ 2′-F dG. Products were cut at U, and the expected sequences began at the 3′ T of the primer.

Product sequence	*m/z*, observed (charge)	*m/z*, theoretical (charge)	Relative peak area/t_R (min)	%
5′-pTCATGA	934.27 (−2)	1,870.22 (−1), 934.60 (−2)	5,585.4/1.68	85
5′-pTCATGAT	1,086.26 (−2), 724.07 (−3)	1,086.70 (−2), 724.13 (−3)	1,838.2/1.91	
5′-pTCAT	613.22 (−2)	1,227.80 (−1), 613.39 (−2)	13,511/1.73	
5′-pTACTGA	934.27 (−2)	1,870.22 (−1), 934.60 (−2)	620.6/1.68	10
5′-pTAGTCAT	1,086.26 (−1), 724.07 (−2)	1,086.70 (−1), 724.13 (−2)	2,095.5/1.91	
5′-pT**G**ATCAT	1,086.26 (−1), 724.07 (−2)	1,086.70 (−1), 724.13 (−2)	1,397/1.91	5

any biological effects cannot be simply ascribed to abasic sites and N^7-CH$_3$ FAPY dG.

N^7-CH$_3$ dG is a substrate for several glycosylases, in addition to removal due to nonenzymatic depurination (53, 54), including 3-alkyladenine DNA glycosylase (AAG) in humans and the bacterial homologs 3-methyladenine glycosylase (AlkA), *Bacillus cereus* DNA glycosylase AlkD, and *Streptomyces sahachiroi* AlkZ (55–57). The chemical and biological half-lives of N^7-CH$_3$ dG have been estimated to be in the range of 69–192 h at 37 °C and neutral pH (chemical) (17) and 29–58 h (biphasic) in rat liver (presumably converting to an abasic site in the study cited, in that N^7-CH$_3$ dG was not detected (49). N^7-CH$_3$ FAPY dG is also a substrate for *Escherichia coli* FPG and other glycosylases (*e.g.* human OGG1, NTH1, and NEIL1) (58–61). The point made here is that N^7-CH$_3$ dG is persistent enough to be copied and miscoded, at least in tissues undergoing DNA replication.

In *E. coli*, N^7-CH$_3$ FAPY dG was not highly mutagenic when bypassed (G to T transversion mutation frequency of ≤2%) (62). When N^7-CH$_3$ FAPY dG was bypassed in a shuttle vector in simian kidney COS-7 cells, it readily produced G to T transversion mutations with 30% frequency (63). N^7-CH$_3$ FAPY dG

Table 5
LC-ESI-MS/MS analysis of full-length extension products across N^7-CH_3 2′-F dG by Dpo4
The oligonucleotides used were as follows,

5′-FAM-CGGGCTCGTAAGCGTCUT- 3′
3′-GCCCGAGCATTCGCAGTA**X**TACT-5′

where **X** represents 2′-F dG and N^7-CH_3 2′-F dG. Products were cut at U, and expected sequences began at 3′ T.

Product sequence	*m/z*, observed (charge)	*m/z*, theoretical (charge)	Relative peak area/t_R (min)	%
5′-pTCATGA	934.22 (−2)	1,870.22 (−1), 934.60 (−2)	6,417/ 1.67	100
5′-pTCATG	777.56 (−2)	1,557.01 (−1), 777.99 (−2)	10,707/1.57	
5′-pTCAT	613.09 (−2)	1,227.80 (−1), 613.39 (−2)	12,253/1.73	

was a strong block to replicative polymerases (*e.g.* pol α and pol δ/proliferating cell nuclear antigen), but hpol η, hpol κ, and the sequential action of hRev1/hpol ζ and Dpo4 were able to bypass N^7-CH_3 FAPY dG (29, 30). With hpol κ, N^7-CH_3 FAPY dG reduced the efficiency of dCTP insertion by an order of magnitude (29). Our previous work on the miscoding properties of N^7-CH_3 FAPY dG (29, 30) can be summarized and compared with the present work on N^7-CH_3 dG. Steady-state kinetic experiments on misinsertion showed only a low frequency of miscoding with *S. solfataricus* Dpo4 (0.01–0.04) but higher frequencies (0.28 and 0.29 for dT and dG insertion, respectively) with *E. coli* DNA polymerase I Klenow fragment. LC-MS analysis showed only misincorporation of dA for both polymerases examined with levels of misincorporation (2–35%) but considerable −1 frameshifts (11–17%) (30). In a later study with mammalian translesion DNA polymerases (29), we observed 2–5% misincorporation at N^7-CH_3 FAPY dG in steady-state kinetics and 11–29% misincorporation by LC-MS for extension products with hpol κ and η. Thus, the extents of misinsertion of hpol η (Tables 1 and 4) are similar in magnitude to those seen with N^7-CH_3 FAPY dG (29), although the oligonucleotide sequence is not the same.

Although Dpo4 and hpol κ are sometimes considered homologs (64, 65), they showed different abilities to replicate past N^7-CH_3 2′-F dG (Fig. 1, *B* and *D*), with hpol κ strongly blocked at the adduct site. hpol κ has been shown to bypass DNA adducts formed with methyl methanesulfonate more efficiently than hpols η and ι, and it also interacts directly with the ligase SHPRH to suppress methyl methanesulfonate–induced mutagenesis (66). hpol ι, which also inserted only dCTP, is also effective in inserting dNTPs across minor groove lesions, such as N^3-methyl deoxyadenosine (67).

Koag *et al.* (37) evaluated the kinetics of insertion of dCTP and dTTP across N^7-CH_3 2′-F dG by pol β, a gap-filling X-family polymerase. The lesion decreased the rate of pol β catalysis by ~300-fold, yet replication was accurate, and no misinsertion products were reported. The structures revealed Watson–Crick base pairing of N^7-CH_3 2′-F dG with an incoming dCTP, but the metal ion coordination was not optimal for catalysis. When N^7-CH_3 2′-F dG was crystallized with dTTP, an open conformation was found, with a staggered bp.

The relatively low but finite level of misincorporation at the N^7-CH_3 dG might seem unimportant. However, consideration needs to be given to the overall mutagenic load. In four different studies cited by Den Engelse *et al.* (49), the ratio of N^7-CH_3 dG to O^6-CH_3 dG adducts following treatment (of cells or rats) with dimethylnitrosamine or methylnitrosoureas was ~10:1. In our own studies with hpol η (68), miscoding in the LC-MS assays was 77%, which may be compared with 15% here with N^7-CH_3 2′-F dG (Table 4). Multiplying the adduct level differences, 77 × 0.1 = 7.7 (O^6-CH_3 dG), which can be compared with 15 × 1 = 15 (N^7-CH_3 (2′-F) dG). Kunkel (43) has estimated a 200–3,000-fold difference in endogenous cellular levels of N^7-CH_3 dG over O^6-CH_3 dG. In a more recent study with cultured human lymphoblastoid cells, Sharma *et al.* (69) reported a 12-fold higher level of N^7-CH_3 dG adducts than O^6-CH_3 dG after treatment with methylnitrosourea and a 900-fold higher level of N^7-CH_3 dG in the untreated cells. Applying the difference in levels of miscoding to these levels of the adducts can therefore result in an even larger potential contribution of N^7-CH_3 dG to miscoding and mutagenesis.

In summary, we have shown that hpol η produces error-free bypass products in copying past N^7-CH_3 2′-F dG and also misinserts dA and dG, differing from the products seen for N^7-CH_3 FAPY dG, which inserted dT and produced a frameshift mutation (29). Our findings indicate that our results are not due to any contamination by the FAPY degradation product and also suggest N^7-CH_3 dG contribution to mutagenicity in cells. Caveats need to be considered about comparing miscoding frequencies in different sequence contexts, the potential roles of DNA polymerases that were not included here, rates of enzymatic repair in different cells, and possibly other issues. Inserting plasmid vectors containing N^7-CH_3 dG into cells to estimate mutation frequencies would be very problematic in terms of being sure that the lesion, even with the 2′-F group, was not modified before mutation occurred. In conclusion, the abundance of the adduct N^7-CH_3 dG, coupled with the evidence for miscoding, argues that this lesion should no longer be considered innocuous.

Experimental procedures

Materials

All chemicals and solvents were commercially available, of highest purity grade, and were used without additional purification. 9-(2-Deoxy-2-fluoro-β-D-arabinofuranosyl) guanine was purchased from Metkinen (Kuopio, Finland). Pyridine, *N*,*N*-dimethylformamide, dichloromethane, *N*,*N*-diisopropylethylamine, isobutyryl chloride, chlorotrimethylsilane, and 4,4′-dimethoxytrityl chloride were purchased from Sigma-Aldrich. Synthesis was monitored by TLC on Merck silica gel 60 F254 plates, with visualization at 254 nm and by spraying a solution of 5% concentrated H_2SO_4 in ethanol (v/v) and heat-

ASBMB

ing. Restriction endonucleases, UDG, FPG glycosylase, dNTPs, and T4 polynucleotide kinase were purchased from New England Biolabs (Ipswich, MA). Unmodified oligonucleotides and primers used for extension and steady-state kinetics were obtained from Integrated DNA Technologies (Coralville, IA) and were HPLC-purified. Primers used for LC-MS sequence analysis were also obtained from DNA Technologies (Coralville, IA) and were twice HPLC-purified. Human DNA polymerases hpol η (catalytic core residues 1–432), hpol ι (catalytic core residues 1–420), and hpol κ (catalytic core residues 19–526) and bacterial Dpo4 were expressed in *E. coli* and purified as described previously (70–73).

NMR spectroscopy and MS

^{1}H and ^{13}C NMR spectra were recorded on a 600-MHz Bruker NMR spectrometer; ^{31}P NMR spectra were recorded on a 500-MHz Bruker NMR spectrometer. Mass spectrometry was performed at the Vanderbilt Mass Spectrometry Research Core Facility using both Thermo low-resolution (LTQ) and high-resolution (Orbitrap) spectrometers. Spectra of synthetic products (negative and positive ion modes) and modified oligonucleotides (negative ion mode) were obtained using a Waters Acquity UPLC instrument (Waters, Milford, MA) interfaced to a Thermo-Finnigan LTQ mass spectrometer (Thermo Scientific, San Jose, CA), also equipped with an electrospray source.

Synthesis of 9-(2-deoxy-2-fluoro-β-D-arabinofuranosyl)-1,9-dihydro-N^2-isobutyrylguanosine (isobutyrylacetamido-6H-purin-6-one) (74)

Commercially available 9-(2-deoxy-2-fluoro-β-D-arabinofuranosyl) guanine (1) (10 mg, 1.05 mmol) was co-evaporated to dryness with anhydrous pyridine (3 × 10 ml) *in vacuo*. The residue was redissolved in anhydrous pyridine (10 ml) solution under an argon atmosphere, and chlorotrimethylsilane (334 μl, 7.88 mmol) was added. The mixture was stirred at room temperature for 2 h and then cooled to 0 °C. Isobutyryl chloride (110 μl, 3.15 mmol) was added in a dropwise manner over 20 min (74). The reaction mixture was allowed to warm to room temperature and further stirred for 3 h. The reaction mixture was then cooled to 0 °C, and water (10 ml) was added to quench the reaction. The reaction was stirred consecutively for 5 min at 0 °C and 5 min at room temperature, and then concentrated aqueous NH_4OH (25 ml) was added, with more stirring for 30 min. H_2O (170 ml) was added to dilute the reaction mixture, and the mixture was extracted with CH_2Cl_2 (50 ml). The aqueous phase was evaporated *in vacuo* to obtain a white solid, 9-(2-deoxy-2-fluoro-β-D-arabinofuranosyl)-N^2-isobubutyryl-guanosine (100 mg, 80%). ^{1}H NMR (DMSO-d_6): δ 8.10 (d, 1H, J = 2.0 Hz, H-8), 6.24 (dd, 1H, J = 4.2, 14.9 Hz, H-1′), 5.18 (dt, 1H, J = 4.2 Hz, 52 Hz, H-2′), 4.38 (dt, 1H, J = 4.2, 17.2 Hz, H-3′), 3.89 (dd, J = 4.9, 10.4 Hz, H-4′), 3.63 (m, 2H, J = 40.26 Hz, H-5′), 2.75 (m, 1H, J = 6.9 Hz, H-11), 1.08 (d, 6H, J = 6.62 Hz, H-12). ^{13}C NMR (DMSO-d_6): 180.8, 155.5, 148.8, 138.8, 120.1, 96.0, 94.8, 84.4, 82.3, 73.0, 60.9, 35.4, 19.5. MS: calculated for $C_{14}H_{18}FN_5O_5$ (M-H) 354.1; found 354.3.

Synthesis of 9-(2-deoxy-2-fluoro-β-D-arabinofuranosyl)-1,9-dihydro-N^7-methyl-N^2-isobutyrylacetamido-6H-purin-6-one (32)

To an anhydrous solution of *N,N*-dimethylformamide (5 ml) was added 9-(2-deoxy-2-fluoro-β-D-arabinofuranosyl)-1,9-dihydro-N^2-isobutyrylguanosine (120 mg, 0.34 mmol) and methyl iodide (351 μl, 5.63 mmol) under an argon atmosphere. The reaction mixture was stirred at room temperature for 22 h and then poured into cold diethyl ether to precipitate the product, which was filtered and concentrated *in vacuo* to afford a white solid, 9-(2-deoxy-2-fluoro-β-D-arabinofuranosyl)-1,9-dihydro-N^2- isobutyryacetamido-6*H*-purin-6-one (114 mg, 80%). ^{1}H NMR (DMSO-d_6): δ 9.69 (s, 1H, H-8), 6.28 (dd, 1H, J = 2.9, 13.8 Hz, H-1′), 5.88 (s, OH), 5.24 (d, 1H, J = 52 Hz, H-2′), 4.96 (s, OH), 4.40 (d, 1H, J = 17.2 Hz, H-3′) 4.08 (s, 3H, N^7-CH_3), 3.98 (s, H-4′), 3.61 (s, 2H, H-5′), 2.69 (t, 1H, J = 7.2 Hz, 13.6 Hz, H-11), 1.04 (d, 6H, J = 6.62 Hz, H-12). ^{13}C NMR (DMSO-d_6): 180.8, 155.5, 148.8, 138.8, 120.1, 96.0, 94.8, 84.4, 82.3, 73.0, 60.9, 35.4, 19.5. MS: calculated for $C_{15}H_{21}FN_5O_5$ (MH^+) 370.2; found 370.2.

Synthesis of 9-[2-deoxy-5-O-(4,4′-dimethoxytrityl)-2-fluoro-β-D-arabinofuranosyl]-1,9-dihydro-N^7-methyl-N^2-isobutyrylacetamido-6H-purin-6-one

9-(2-Deoxy-2-fluoro-β-D-arabinofuranosyl)-1,9-dihydro-N^7-methyl-N^2- isobutyryacetamido-6*H*-purin-6-one (263 mg, 0.71 mmol), in anhydrous pyridine, and 4,4′-dimethoxytrityl chloride (721 mg, 2.1 mmol) were stirred at room temperature for 2 h under an argon atmosphere. The reaction mixture was diluted with CH_2Cl_2 (50 ml) and washed with saturated aqueous $NaHCO_3$ and then brine (3 × 50 ml). The organic layer was dried over anhydrous Na_2SO_4 and filtered, and the solvent was evaporated. The crude residue was purified by silica gel column chromatography (3% CH_3OH in CH_2Cl_2 plus 1% triethylamine, v/v) to afford 9-[2-deoxy-5-*O*-(4,4′-dimethoxytrityl)-2-fluoro-β-D-arabinofuranosyl]-1,9-dihydro-N^7-methyl-N^2-isobutyrylacetamido-6*H*-purin-6-one (290 mg, 60% yield). ^{1}H NMR (600 MHz, CD_2Cl_2): δ 8.44 (1H, s, H-8), 6.93–7.52 (13H, m, aromatic H), 6.86 (1H, d, J = 7.7 Hz, H-1′), 5.34 (1H, t, 2.8, H-2′), 4.72 (1H, d, J = 17.22 Hz, H-3′), 4.45 (1H, m, H-4′), 3.97 (3H, s, N^7-CH_3), 3.79 (6H, s, OCH_3, OCH_3), 3.49–3.56 (2H, m, 7.27, 5.25 Hz, H-5 and H-5′), 2.72 (1H, m, H11), 1.109 (dd, 6H, J = 1.82, 11.62 Hz, H-12). MS: calculated for $C_{36}H_{39}FN_5O_7$ (MH^+) 672.3; found 672.2.

Synthesis of 9-[2-deoxy-5-O-(4,4′-dimethoxytrityl)-2-fluoro-β-D-arabinofuranosyl]-1,9-dihydro-N^7-methyl-N^2-isobutyrylacetamido-6H-purin-6-one-3-O-(2-cyanoethyl)-N,N-diisopropylphosphoramidite

The dimethoxytrityl-protected nucleoside from the previous step (90 mg, 134 μmol) was dissolved in CH_2Cl_2 (2 ml), and *N,N*-diisopropyethylamine (55 μl, 0.33 mmol) was added. *N,N*-Diisopropylamino)chlorophosphine (45 μl, 0.2 mmol) was added, and then the reaction mixture was stirred at room temperature for 2 h under an argon atmosphere. The mixture was diluted with CH_2Cl_2 (50 ml) and washed with saturated aqueous $NaHCO_3$ and then brine (3 × 50 ml), and the organic phase was dried over Na_2SO_4 and filtered. The solvent was evaporated

in vacuo. The crude reaction mixture was purified by silica gel chromatography with 1% CH_3OH in CH_2Cl_2 containing 1% trimethylamine (v/v) to afford 80 mg of 9-[2-deoxy-5-*O*-(4,4′-dimethoxytrityl)-2-fluoro-β-D-arabinofuranosyl]-1,9-dihydro-N^7-methyl-N^2-isobutyrylacetamido-6*H*-purin-6-one-3-*O*-(2-cyanoethyl)-*N*,*N*-diisopropylphosphoramidite, 68%. ^{31}P NMR (500 MHz, CD_2Cl_2) δ 152.48, 152.30; MS: calculated for $C_{36}H_{39}FN_5O_7$ (MH^+) 872.4; found 872.4.

Synthesis, purification, and characterization of 2′-F dG and N^7-CH_3 2′-F dG–containing DNA oligonucleotides

Modified oligonucleotides bearing 2′-fluorines were synthesized with Expedite reagents (Glen Research, Sterling, VA) on a 1-μmol scale utilizing a Perspective Biosystems model 8909 DNA synthesizer and a standard synthetic protocol (75). We chose the β-anomer for the 2′-fluoro analogs because this configuration has been shown not to alter sugar puckering in DNA; this is the typical configuration for the 2′-deoxynucleotides (76–78). The coupling of N^7-CH_3 2′-F dG phosphoramidite was performed off-line for 2 h. The remainder of the synthesis was done online using standard procedures. Modified oligonucleotides were cleaved from the solid support, and exocyclic groups were deprotected in a single step using anhydrous methanolic K_2CO_3 (50 mM), stirring at room temperature for 8 h. CH_3OH was removed by sweeping with a stream of N_2 gas. Oligonucleotides were purified by reversed-phase HPLC with a Phenominex Alumina RP octadecylsilane (C_{18}) column (250 mm × 4.6 mm, 5 μm). The solvents used were aqueous 100 mM triethylammonium acetate (mobile phase A) and 100 mM triethylammonium acetate in H_2O/CH_3CN (1:1, v/v) (mobile phase B). The flow rate was 1.5 ml/min with the following gradient: initial 20% B, increased to 25% B over 5 min, held at 25% for 15 min, increased to 40% at 20 min, held for 5 min, then 100% at 25 min, and held until 30 min and 5% B at 31 min and re-equilibrated to 0% B for 5 min (all v/v). The UV detector was set at 240 nm. The collected fractions were lyophilized to dryness, redissolved in water, and desalted using ZipTip U-C18 columns prior to characterization.

Oligonucleotide 5′-TCAT(2′-F dG) ATGACGCTTACGAGCCCG-3′ was purified by HPLC, LC-ESI *m/z* calculated for $[M-H]^-$, 7039.193; found 7043.000 (Fig. S5*B*).

Oligonucleotide 5′-TCAT(N^7-CH_3 2′-F dG)ATGACGCTTACGAGCCCG-3′ was purified by HPLC, LC-ESI *m/z* calculated for $[M-H]^-$, 7054.216; found 7075.000 (Fig. S6*A*) (presumably sodium adduct).

The identity of the N^7-CH_3 2′-F dG–containing oligonucleotide was further confirmed by subjecting it to FPG glycosylase. The N^7-CH_3 2′-F dG–containing oligonucleotide was ^{32}P-labeled at the 5′-end using T4 polynucleotide kinase (New England Biolabs) and annealed to its complementary strand by heating at 95 °C for 5 min and then allowing it to cool to room temperature overnight. A second portion of the N^7-CH_3 2′-F dG-oligonucleotide was treated with NaOH and stirred for 12 h at room temperature to create a hydrolyzed N^7-CH_3 FAPY-2′-F dG oligonucleotide. It was also 5′-end–labeled (^{32}P-label and T4 polynucleotide kinase) and then annealed with its complementary strand. Both oligonucleotides were subjected to treatment with FPG glycosylase for 1 h at 37 °C. Reactions were quenched with 9 μl of quenching dye (20 mM EDTA, (pH 9.0) in 95% formamide, v/v) and the products were separated on a 20% acrylamide (w/v) electrophoresis gel. Results were visualized using a phosphorimaging system (Bio-Rad, Molecular Imager® FX) and analyzed by Quantity One software as described previously (38).

Primer annealing and extension assays

5′-FAM-labeled 16-mer, 18-mer, and 19-mer primers (5′-/FAM/CGGGCTCGTAAGCGTC-3′, 5′-/FAM/CGGGCTCGTAAGCGTCAT-3′, 5′-/FAM/CGGGCTCGTAAGCGTCATC-3′, and 5′-/FAM/CGGGCTCGTAAGCGTCATT-3′, respectively) were annealed to a 23-mer template (3′-GCCCGAGCATTCGCAGTA**X**TACT-5′, where **X** was dG, 2′-F dG, or N^7-CH_3 2′-F dG, in a 1:1 molar ratio at 95 °C for 5 min and slowly cooling to room temperature. For the full-length extension assays, WT hpol η (20 nM), hpol ι (40 nM), hpol κ (20 nM), and Dpo4 (20 nM) were incubated with the 16-mer primer–template DNA complex (200 nM) in 40 mM Tris-HCl buffer (pH 7.5) containing 5 mM $MgCl_2$, 50 mM NaCl, 5% glycerol (v/v), 5 mM DTT, 50 μg/ml BSA, and 250 μM dNTPs. The reactions were done at 37 °C for 2, 5, 10, 20, and 60 min. For single-nucleotide incorporation experiments, an 18-mer primer–template DNA complex (120 nM) was used. Enzyme concentrations were as follows: hpol η (5 nM), hpol ι (10 nM), hpol κ (5 nM), and Dpo4 (5 nM). Reactions were done for 10 min. In the case of the single-nucleotide extension experiments, two primer–template DNA complexes (120 nM) were used with hpol η (5 nM) alone for 5 min. All other reaction conditions were the same as in the full-length extension experiments. Reactions were quenched as above, and products were separated on 18% denaturing acrylamide gels (w/v) and visualized with a Typhoon system (GE Healthcare).

Steady-state insertion and extension kinetics

Insertion reactions were done by incubating FAM-labeled 18-mer primer/23-mer template complexes (120 nM) with hpol η (2.5–10 nM) or Dpo4 (0.15–10 nM), and extension reactions were conducted by incubating two FAM-labeled 19-mer primer/23-mer template complexes (120 nM) with hpol η (5–10 nM). Both reactions were incubated at 37 °C for 5–10 min in 50 mM Tris-HCl buffer (pH 7.5) containing 5 mM $MgCl_2$, 50 mM NaCl, 5% glycerol (v/v), 5 mM DTT, 50 μg/ml BSA, and varying concentrations of dNTPs. Reactions were quenched as described above, and products were separated on 18% denaturing acrylamide gels (w/v), visualized with a Typhoon system, and quantified utilizing ImageJ software (National Institutes of Health). Data obtained were fit to the hyperbolic Michaelis–Menten equation in GraphPad Prism software (version 8.0, La Jolla, CA).

LC-MS analysis of full-length extension products by hpol η and Dpo4

An 18-mer primer bearing a 2′-deoxyuridine (5′-FAM/CGGGCTCGTAAGCGTC(dU)T-3′) was annealed to the 23-mer oligomer used above, in a molar ratio of 1:1. Full-length extension reactions were done using similar conditions as in the steady-state experiments, with the exception of primer–

template complex (2.5 μM), hpol η (150 nM), Dpo4 (300 nM), and dNTPs (500 μM). Reactions were incubated at 37 °C for 1 h. Reactions were quenched by spin column separation to remove Mg^{2+} and dNTPs, and the extension product was treated with 25 units of UDG at 37 °C for 4 h and then with 0.25 M piperidine, heating at 95 °C for 1 h. H_2O was added to the reaction mixture, which was lyophilized and then redissolved in H_2O (70). Products were analyzed by LC-MS/MS, performed using a Waters Acquity UPLC system linked to a Thermo-Finnigan LTQ mass spectrometer with electrospray ionization in the negative ion mode. Separation by chromatography was done using an Acquity UPLC system BEH octadecylsilane (C_{18}) column (1.7 μm, 2.1 mm × 50 mm) with UPLC conditions as described previously (40).

Author contributions—F. P. G. conceived the studies; Y. S. expressed and purified hpol η; F. P. G. and O. J. N. designed the experiments, interpreted the data, and wrote the manuscript; O. J. N. carried out organic synthesis, characterization of the oligonucleotides, steady-state kinetics, and LC-MS sequence analysis.

Acknowledgments—We thank Drs. Carmelo J. Rizzo and Chanchal Malik for DNA synthesis and helpful discussions, Dr. Carl A. Sedgeman for helpful suggestions, and Dr. Plamen P. Christov for help with LC-MS sequencing analysis. Mass spectrometry was performed at the Vanderbilt Mass Spectrometry Research Core Facility. We also thank K. Trisler for assistance with preparation of the manuscript.

References

1. Swenberg, J. A., Lu, K., Moeller, B. C., Gao, L., Upton, P. B., Nakamura, J., and Starr, T. B. (2011) Endogenous *versus* exogenous DNA adducts: their role in carcinogenesis, epidemiology, and risk assessment. *Toxicol. Sci.* **120,** S130–S145 CrossRef Medline
2. Helleday, T., Eshtad, S., and Nik-Zainal, S. (2014) Mechanisms underlying mutational signatures in human cancers. *Nat. Rev. Genet.* **15,** 585–598 CrossRef Medline
3. Weismann, C. G., and Gelb, B. D. (2007) The genetics of congenital heart disease: a review of recent developments. *Curr. Opin. Cardiol.* **22,** 200–206 CrossRef Medline
4. Shigenaga, M. K., Hagen, T. M., and Ames, B. N. (1994) Oxidative damage and mitochondrial decay in aging. *Proc. Natl. Acad. Sci. U.S.A.* **91,** 10771–10778 CrossRef Medline
5. Sedgwick, B. (2004) Repairing DNA-methylation damage. *Nat. Rev. Mol. Cell Biol.* **5,** 148–157 CrossRef Medline
6. Erickson, R. P. (2003) Somatic gene mutation and human disease other than cancer. *Mut. Res.* **543,** 125–136 CrossRef Medline
7. Newell, D., Gescher, A., Harland, S., Ross, D., and Rutty, C. (1987) *N*-Methyl antitumour agents: a distinct class of anticancer drugs? *Cancer Chemother. Pharmacol.* **19,** 91–102 Medline
8. Friedman, H. S., Kerby, T., and Calvert, H. (2000) Temozolomide and treatment of malignant glioma. *Clin. Cancer Res.* **6,** 2585–2597 Medline
9. Lidor, Y. J., Shpall, E. J., Peters, W. P., and Bast, R. C., Jr. (1991) Synergistic cytotoxicity of different alkylating agents for epithelial ovarian cancer. *Int. J. Cancer* **49,** 704–710 CrossRef Medline
10. McGuire, W. P., 3rd, and Markman, M. (2003) Primary ovarian cancer chemotherapy: current standards of care. *Br. J. Cancer* **89,** S3–S8 CrossRef Medline
11. Dolan, M. E., McRae, B. L., Ferries-Rowe, E., Belanich, M., van Seventer, G. A., Guitart, J., Pezen, D., Kuzel, T. M., and Yarosh, D. B. (1999) O^6-Alkylguanine-DNA alkyltransferase in cutaneous T-cell lymphoma: implications for treatment with alkylating agents. *Clin. Cancer Res.* **5,** 2059–2064 Medline
12. Lindahl, T. (1993) Instability and decay of the primary structure of DNA. *Nature* **362,** 709–715 CrossRef Medline
13. Beranek, D. T. (1990) Distribution of methyl and ethyl adducts following alkylation with monofunctional alkylating agents. *Mut. Res.* **231,** 11–30 CrossRef
14. Newbold, R. F., Warren, W., Medcalf, A. S., and Amos, J. (1980) Mutagenicity of carcinogenic methylating agents is associated with a specific DNA modification. *Nature* **283,** 596–599 CrossRef Medline
15. Mitra, G., Pauly, G. T., Kumar, R., Pei, G. K., Hughes, S. H., Moschel, R. C., and Barbacid, M. (1989) Molecular analysis of O^6-substituted guanine-induced mutagenesis of *ras* oncogenes. *Proc. Natl. Acad. Sci. U.S.A.* **86,** 8650–8654 CrossRef Medline
16. Pullman, A., and Pullman, B. (1981) Molecular electrostatic potential of the nucleic acids. *Q. Rev. Biophys.* **14,** 289–380 CrossRef Medline
17. Gates, K. S., Nooner, T., and Dutta, S. (2004) Biologically relevant chemical reactions of N^7-alkylguanine residues in DNA. *Chem. Res. Toxicol.* **17,** 839–856 CrossRef Medline
18. Kou, Y., Koag, M. C., and Lee, S. (2018) Structural and kinetic studies of the effect of guanine N7 alkylation and metal cofactors on DNA replication. *Biochemistry* **57,** 5105–5116 CrossRef Medline
19. Bailey, E. A., Iyer, R. S., Stone, M. P., Harris, T. M., and Essigmann, J. M. (1996) Mutational properties of the primary aflatoxin B_1-DNA adduct. *Proc. Natl. Acad. Sci. U.S.A.* **93,** 1535–1539 CrossRef Medline
20. Brookes, P., and Lawley, P. D. (1960) The reaction of mustard gas with nucleic acids *in vitro* and *in vivo*. *Biochem. J.* **77,** 478–484 CrossRef Medline
21. Boysen, G., Pachkowski, B. F., Nakamura, J., and Swenberg, J. A. (2009) The formation and biological significance of N^7-guanine adducts. *Mutat. Res.* **678,** 76–94 CrossRef Medline
22. Williams, J. S., and Kunkel, T. A. (2014) Ribonucleotides in DNA: origins, repair and consequences. *DNA Repair* (*Amst.*) **19,** 27–37 CrossRef Medline
23. Caldecott, K. W. (2014) Molecular biology. Ribose–an internal threat to DNA. *Science* **343,** 260–261 CrossRef Medline
24. Mustonen, R., and Hemminki, K. (1992) 7-Methylguanine levels in DNA of smokers' and non-smokers' total white blood cells, granulocytes and lymphocytes. *Carcinogenesis* **13,** 1951–1955 CrossRef Medline
25. Park, J. W., and Ames, B. N. (1988) 7-Methylguanine adducts in DNA are normally present at high levels and increase on aging: analysis by HPLC with electrochemical detection. *Proc. Natl. Acad. Sci. U.S.A.* **85,** 7467–7470 CrossRef Medline
26. Barrows, L. R., and Magee, P. N. (1982) Nonenzymatic methylation of DNA by *S*-adenosylmethionine *in vitro*. *Carcinogenesis* **3,** 349–351 CrossRef Medline
27. Yu, S. L., Lee, S. K., Johnson, R. E., Prakash, L., and Prakash, S. (2003) The stalling of transcription at abasic sites is highly mutagenic. *Mol. Cell. Biol.* **23,** 382–388 CrossRef Medline
28. Gibbs, P. E., and Lawrence, C. W. (1995) Novel mutagenic properties of abasic sites in *Saccharomyces cerevisiae*. *J. Mol. Biol.* **251,** 229–236 CrossRef Medline
29. Christov, P. P., Yamanaka, K., Choi, J.-Y., Takata, K., Wood, R. D., Guengerich, F. P., Lloyd, R. S., and Rizzo, C. J. (2012) Replication of the 2,6-diamino-4-hydroxy-N^5-methyl-formamidopyrimidine (MeFapy-dGuo) adduct by eukaryotic DNA polymerases. *Chem. Res. Toxicol.* **25,** 1652–1661 CrossRef Medline
30. Christov, P. P., Angel, K. C., Guengerich, F. P., and Rizzo, C. J. (2009) Replication past the N^5-methyl-formamidopyrimidine lesion of deoxyguanosine by DNA polymerases and an improved procedure for sequence analysis of *in vitro* bypass products by mass spectrometry. *Chem. Res. Toxicol.* **22,** 1086–1095 CrossRef Medline
31. Dizdaroglu, M., Kirkali, G., and Jaruga, P. (2008) Formamidopyrimidines in DNA: mechanisms of formation, repair, and biological effects. *Free Radic. Biol. Med.* **45,** 1610–1621 CrossRef Medline
32. Lee, S., Bowman, B. R., Ueno, Y., Wang, S., and Verdine, G. L. (2008) Synthesis and structure of duplex DNA containing the genotoxic nucleobase lesion N^7-methylguanine. *J. Am. Chem. Soc.* **130,** 11570–11571 CrossRef Medline

33. Barbin, A., Laib, R. J., and Bartsch, H. (1985) Lack of miscoding properties of 7-(2-oxoethyl)guanine, the major vinyl chloride-DNA adduct. *Cancer Res.* **45,** 2440–2444 Medline
34. Lawley, P. D., and Brookes, P. (1961) Acidic dissociation of 7:9-dialkylguanines and its possible relation to mutagenic properties of alkylating agents. *Nature* **192,** 1081–1082 CrossRef Medline
35. Sowers, L. C., Shaw, B. R., Veigl, M. L., and Sedwick, W. D. (1987) DNA base modification: ionized base pairs and mutagenesis. *Mutat. Res.* **177,** 201–218 CrossRef Medline
36. Lawley, P. D., and Brookes, P. (1962) Ionization of DNA bases or base analogues as a possible explanation of mutagenesis, with special reference to 5-bromodeoxyuridine. *J. Mol. Biol.* **4,** 216–219 CrossRef Medline
37. Koag, M. C., Kou, Y., Ouzon-Shubeita, H., and Lee, S. (2014) Transition-state destabilization reveals how human DNA polymerase β proceeds across the chemically unstable lesion N^7-methylguanine. *Nucleic Acids Res.* **42,** 8755–8766 CrossRef Medline
38. Zhao, L., Christov, P. P., Kozekov, I. D., Pence, M. G., Pallan, P. S., Rizzo, C. J., Egli, M., and Guengerich, F. P. (2012) Replication of N^2,3-ethenoguanine by DNA polymerases. *Angew. Chem. Int. Ed. Engl.* **51,** 5466–5469 CrossRef Medline
39. Lawley, P. D. (1984) Carcinogenesis by alkylating agents. In *Chemical Carcinogens*, 2nd Ed. (Searle, C. E., ed) pp. 324–484, American Chemical Society, Washington, D. C.
40. Sedgeman, C. A., Su, Y., and Guengerich, F. P. (2017) Formation of *S*-[2-(N^6-deoxyadenosinyl)ethyl]glutathione in DNA and replication past the adduct by translesion DNA polymerases. *Chem. Res. Toxicol.* **30,** 1188–1196 CrossRef Medline
41. Watson, J. D., and Crick, F. H. C. (1953) Genetical implications of the structure of deoxyribonucleic acid. *Nature* **171,** 964–967 CrossRef Medline
42. Lawley, P. D., and Orr, D. J. (1970) Specific excision of methylation products from DNA of *Escherichia coli* treated with *N*-methyl-*N*′-nitro-*N*-nitrosoguanidine. *Chem. Biol. Interact.* **2,** 154–157 CrossRef Medline
43. Kunkel, T. A. (1999) The high cost of living. American Association for Cancer Research Special Conference: Endogenous sources of mutations. *Trends Genet.* **15,** 93–94 CrossRef Medline
44. De Bont, R., and van Larebeke, N. (2004) Endogenous DNA damage in humans: a review of quantitative data. *Mutagenesis* **19,** 169–185 CrossRef Medline
45. Inskeep, P. B., Koga, N., Cmarik, J. L., and Guengerich, F. P. (1986) Covalent binding of 1,2-dihaloalkanes to DNA and stability of the major DNA adduct, *S*-[2-(N^7-guanyl)ethyl]glutathione. *Cancer Res.* **46,** 2839–2844 Medline
46. Humphreys, W. G., and Guengerich, F. P. (1991) Structure of formamidopyrimidine adducts as determined by NMR using specifically ^{15}N-labeled guanosine. *Chem. Res. Toxicol.* **4,** 632–636 CrossRef Medline
47. Mao, H., Deng, Z., Wang, F., Harris, T. M., and Stone, M. P. (1998) An intercalated and thermally stable FAPY adduct of aflatoxin B_1 in a DNA duplex: structural refinement from ^{1}H NMR. *Biochemistry* **37,** 4374–4387 CrossRef Medline
48. Hendler, S., Fürer, E., and Srinivasan, P. R. (1970) Synthesis and chemical properties of monomers and polymers containing 7-methylguanine and an investigation of their substrate or template properties for bacterial deoxyribonucleic acid or ribonucleic acid polymerase. *Biochemistry* **9,** 4141–4153 CrossRef Medline
49. Den Engelse, L., Menkveld, G. J., De Brij, R. J., and Tates, A. D. (1986) Formation and stability of alkylated pyrimidines and purines (including imidazole ring-opened 7-alkylguanine) and alkylphosphotriesters in liver DNA of adult rats treated with ethylnitrosourea or dimethylnitrosamine. *Carcinogenesis* **7,** 393–403 CrossRef Medline
50. Beranek, D. T., Weis, C. C., Evans, F. E., Chetsanga, C. J., and Kadlubar, F. F. (1983) Identification of N^5-methyl-N^5-formyl-2,5,6-triamino-4-hydroxypyrimidine as a major adduct in rat liver DNA after treatment with the carcinogens, *N*,*N*-dimethylnitrosamine or 1,2-dimethylhydrazine. *Biochem. Biophys. Res. Commun.* **110,** 625–631 CrossRef Medline
51. Kadlubar, F. F., Beranek, D. T., Weis, C. C., Evans, F. E., Cox, R., and Irving, C. C. (1984) Characterization of the purine ring-opened 7-methylguanine and its persistence in rat bladder epithelial DNA after treatment with the carcinogen *N*-methylnitrosourea. *Carcinogenesis* **5,** 587–592 CrossRef Medline
52. Oida, T., Humphreys, W. G., and Guengerich, F. P. (1991) Preparation and characterization of oligonucleotides containing *S*-[2-(N^7-guanyl)ethyl-]glutathione. *Biochemistry* **30,** 10513–10522 CrossRef Medline
53. Xiao, W., and Samson, L. (1993) *In vivo* evidence for endogenous DNA alkylation damage as a source of spontaneous mutation in eukaryotic cells. *Proc. Natl. Acad. Sci. U.S.A.* **90,** 2117–2121 CrossRef Medline
54. Barbado, C., Córdoba-Canero, D., Ariza, R. R., and Roldán-Arjona, T. (2018) Nonenzymatic release of N^7-methylguanine channels repair of abasic sites into an AP endonuclease-independent pathway in *Arabidopsis*. *Proc. Natl. Acad. Sci. U.S.A.* **115,** E916–E924 CrossRef Medline
55. Parsons, Z. D., Bland, J. M., Mullins, E. A., and Eichman, B. F. (2016) A catalytic role for C-H/π interactions in base excision repair by *Bacillus cereus* DNA glycosylase AlkD. *J. Am. Chem. Soc.* **138,** 11485–11488 CrossRef Medline
56. Mullins, E. A., Warren, G. M., Bradley, N. P., and Eichman, B. F. (2017) Structure of a DNA glycosylase that unhooks interstrand cross-links. *Proc. Natl. Acad. Sci. U.S.A.* **114,** 4400–4405 CrossRef Medline
57. Hollis, T., Lau, A., and Ellenberger, T. (2000) Structural studies of human alkyladenine glycosylase and *E. coli* 3-methyladenine glycosylase. *Mutat. Res.* **460,** 201–210 CrossRef Medline
58. Asagoshi, K., Yamada, T., Terato, H., Ohyama, Y., Monden, Y., Arai, T., Nishimura, S., Aburatani, H., Lindahl, T., and Ide, H. (2000) Distinct repair activities of human 7,8-dihydro-8-oxoguanine DNA glycosylase and formamidopyrimidine DNA glycosylase for formamidopyrimidine and 7,8-dihydro-8-oxoguanine. *J. Biol. Chem.* **275,** 4956–4964 CrossRef Medline
59. Dherin, C., Radicella, J. P., Dizdaroglu, M., and Boiteux, S. (1999) Excision of oxidatively damaged DNA bases by the human α-hOgg1 protein and the polymorphic α-hOgg1(Ser326Cys) protein which is frequently found in human populations. *Nucleic Acids Res.* **27,** 4001–4007 CrossRef Medline
60. Katafuchi, A., Nakano, T., Masaoka, A., Terato, H., Iwai, S., Hanaoka, F., and Ide, H. (2004) Differential specificity of human and *Escherichia coli* endonuclease III and VIII homologues for oxidative base lesions. *J. Biol. Chem.* **279,** 14464–14471 CrossRef Medline
61. Asagoshi, K., Yamada, T., Okada, Y., Terato, H., Ohyama, Y., Seki, S., and Ide, H. (2000) Recognition of formamidopyrimidine by *Escherichia coli* and mammalian thymine glycol glycosylases: distinctive paired base effects and biological and mechanistic implications. *J. Biol. Chem.* **275,** 24781–24786 CrossRef Medline
62. Patro, J. N., Wiederholt, C. J., Jiang, Y. L., Delaney, J. C., Essigmann, J. M., and Greenberg, M. M. (2007) Studies on the replication of the ring opened formamidopyrimidine, Fapy-dG in *Escherichia coli*. *Biochemistry* **46,** 10202–10212 CrossRef Medline
63. Kalam, M. A., Haraguchi, K., Chandani, S., Loechler, E. L., Moriya, M., Greenberg, M. M., and Basu, A. K. (2006) Genetic effects of oxidative DNA damages: comparative mutagenesis of the imidazole ring-opened formamidopyrimidines (Fapy lesions) and 8-oxo-purines in simian kidney cells. *Nucleic Acids Res.* **34,** 2305–2315 CrossRef Medline
64. Wolfle, W. T., Washington, M. T., Prakash, L., and Prakash, S. (2003) Human DNA polymerase κ uses template-primer misalignment as a novel means for extending mispaired termini and for generating single-base deletions. *Genes Dev.* **17,** 2191–2199 CrossRef Medline
65. Ling, H., Boudsocq, F., Woodgate, R., and Yang, W. (2001) Crystal structure of a Y-family DNA polymerase in action: a mechanism for error-prone and lesion-bypass replication. *Cell* **107,** 91–102 CrossRef Medline
66. Lin, J. R., Zeman, M. K., Chen, J. Y., Yee, M. C., and Cimprich, K. A. (2011) SHPRH and HLTF act in a damage-specific manner to coordinate different forms of postreplication repair and prevent mutagenesis. *Mol. Cell* **42,** 237–249 CrossRef Medline
67. Yoon, J. H., Roy Choudhury, J., Park, J., Prakash, S., and Prakash, L. (2017) Translesion synthesis DNA polymerases promote error-free replication through the minor-groove DNA adduct 3-deaza-3-methyladenine. *J. Biol. Chem.* **292,** 18682–18688 CrossRef Medline
68. Choi, J.-Y., Chowdhury, G., Zang, H., Angel, K. C., Vu, C. C., Peterson, L. A., and Guengerich, F. P. (2006) Translesion synthesis across O^6-alkyl-

guanine DNA adducts by recombinant human DNA polymerases. *J. Biol. Chem.* **281,** 38244–38256 CrossRef Medline

69. Sharma, V., Collins, L. B., Clement, J. M., Zhang, Z., Nakamura, J., and Swenberg, J. A. (2014) Molecular dosimetry of endogenous and exogenous O^6-methyl-dG and N^7-methyl-G adducts following low dose D_3-methylnitrosourea exposures in cultured human cells. *Chem. Res. Toxicol.* **27,** 480–482 CrossRef Medline
70. Zang, H., Goodenough, A. K., Choi, J.-Y., Irimia, A., Loukachevitch, L. V., Kozekov, I. D., Angel, K. C., Rizzo, C. J., Egli, M., and Guengerich, F. P. (2005) DNA adduct bypass polymerization by *Sulfolobus solfataricus* DNA polymerase Dpo4: analysis and crystal structures of multiple base pair substitution and frameshift products with the adduct 1,N^2-ethenoguanine. *J. Biol. Chem.* **280,** 29750–29764 CrossRef Medline
71. Pence, M. G., Choi, J.-Y., Egli, M., and Guengerich, F. P. (2010) Structural basis for proficient incorporation of dTTP opposite O^6-methylguanine by human DNA polymerase ι. *J. Biol. Chem.* **285,** 40666–40672 CrossRef Medline
72. Patra, A., Nagy, L. D., Zhang, Q., Su, Y., Müller, L., Guengerich, F. P., and Egli, M. (2014) Kinetics, structure, and mechanism of 8-oxo-7,8-dihydro-2′-deoxyguanosine bypass by human DNA polymerase η. *J. Biol. Chem.* **289,** 16867–16882 CrossRef Medline
73. Irimia, A., Eoff, R. L., Guengerich, F. P., and Egli, M. (2009) Structural and functional elucidation of the mechanism promoting error-prone synthesis by human DNA polymerase κ opposite the 7,8-dihydro-8-oxo-2′-deoxyguanosine adduct. *J. Biol. Chem.* **284,** 22467–22480 CrossRef Medline
74. Wilson, T. J., Li, N. S., Lu, J., Frederiksen, J. K., Piccirilli, J. A., and Lilley, D. M. (2010) Nucleobase-mediated general acid-base catalysis in the Varkud satellite ribozyme. *Proc. Natl. Acad. Sci. U.S.A.* **107,** 11751–11756 CrossRef Medline
75. Elmquist, C. E., Stover, J. S., Wang, Z., and Rizzo, C. J. (2004) Site-specific synthesis and properties of oligonucleotides containing C8-deoxyguanosine adducts of the dietary mutagen IQ. *J. Am. Chem. Soc.* **126,** 11189–11201 CrossRef Medline
76. Marquez, V. E., Tseng, C. K.-H., Mitsuya, H., Aoki, S., Kelley, J. A., Ford, H., Jr., Roth, J. S., Broder, S., Johns, D. G., and Driscoll, J. S. (1990) Acid-stable 2′-fluoro purine dideoxynucleosides as active agents against HIV. *J. Med. Chem.* **33,** 978–985 CrossRef Medline
77. Schärer, O. D., and Verdine, G. L. (1995) A designed inhibitor of base-excision DNA repair. *J. Am. Chem. Soc.* **117,** 10781–10782 CrossRef
78. Ikeda, H., Fernandez, R., Wilk, A., Barchi, J. J., Jr., Huang, X., and Marquez, V. E. (1998) The effect of two antipodal fluorine-induced sugar puckers on the conformation and stability of the Dickerson-Drew dodecamer duplex $[d(CGCGAATTCGCG)]_2$. *Nucleic Acids Res.* **26,** 2237–2244 CrossRef Medline